Available on the CERN CDS information server **CMS PAS FTR-18-040**

CMS Physics Analysis Summary

Contact: cms-phys-conveners-ftr@cern.ch 2019/02/14

Search for a new scalar resonance decaying to a pair of Z bosons at the High-Luminosity LHC

The CMS Collaboration

Abstract

For a heavy resonance decaying into a pair of Z bosons, a projection of current CMS searches to the HL-LHC is presented. The study considers pp collisions for an integrated luminosity of 3000 fb^{-1} and takes into account the Phase-2 upgrade of the CMS detector. The final state with two leptons and two quarks is used to search for heavy resonances in the mass range from 550 GeV to 3 TeV. The scalar particle X is assumed to have a decay width much narrower than the detector resolution. Upper limits on the cross sections for models predicting the production of this scalar resonance through gluon fusion and electroweak mechanisms are presented.

1 Introduction

The standard model (SM) of particle physics postulates the existence of a single Higgs boson as the manifestation of a scalar field responsible for electroweak (EW) symmetry breaking [1–7]. The ATLAS and CMS Collaborations have discovered a boson with a mass of 125 GeV [8–10] and with properties consistent with those expected for the SM Higgs boson [11–15].To-date there is no experimental evidence for the particles beyond the standard model. Nonetheless, searches for BSM physics are motivated by a number of phenomena such as the presence of dark matter or baryon asymmetry in the universe that are not explained by the SM. The BSM models that attempt to address these questions include two-Higgs-doublet models (2HDM) [16] as predicted by supersymmetry or other models predicting an extended Higgs-like EW singlet [17]. CMS and ATLAS collaborations have performed searches for a heavy scalar partner of the SM Higgs boson decaying into a pair of Z bosons [18, 19]. The ZZ decay has a sizable branching fraction for an SM-like Higgs boson of mass larger than the Z boson pair production threshold, $2m_Z$, and is one of the main discovery channels for masses less than $2m_Z$ [8–10]. The search for a new scalar boson X is performed over a range of masses from 550 GeV up to 3 TeV.

The CMS search for a heavy scalar partner of the SM Higgs boson using 35.9 fb^{-1} of pp collision data [19] will be referred to as Run-2 analysis throughout the article. In Run-2 analysis, the search for a scalar resonance X decaying to ZZ is performed over the mass range $130\,\text{GeV} < m_X < 3\,\text{TeV}$, where three final states based on leptonic or hadronic decays of Z boson, $\text{X} \to \text{ZZ} \to 4\ell$, 2ℓ2q, and $2\ell 2\nu$ are combined. Because of the different resolutions, efficiencies, and branching fractions, each final state contributes differently depending on the signal mass hypothesis. The most sensitive final state for the mass range of 130–500 GeV is 4ℓ due to its best mass resolution, whereas, for the intermediate region of 500–700 GeV, $2\ell 2\nu$ is most sensitive. For masses above 700 GeV 2ℓ2q provides the best sensitivity. In this paper, we are particularly interested in the sensitivity in the high mass region, thus only 2ℓ2q is used.

In the 2ℓ2q final state, events are selected by combining leptonically and hadronically decaying Z candidates. The lepton pairs (electron or muon) of opposite sign and same flavor with invariant mass between 60 and 120 GeV are constructed. Hadronically decaying Z boson candidates (Z_{had}) are reconstructed using two distinct techniques, which are referred to as "resolved" and "merged". In the resolved case, the two quarks from the Z boson decay form two distinguishable narrow jets, while in the merged case a single wide jet with a large p_{T} is taken as a Z_{had}.

An arbitration procedure is used to rank multiple Z_{had} candidates reconstructed in a single event: merged candidates have precedence over resolved candidates if they have $p_{\text{T}} > 300\,\text{GeV}$ and the accompanying leptonically decaying Z candidate has $p_{\text{T}}(\text{L}_{\text{L}}) > 200\,\text{GeV}$; resolved candidates have precedence otherwise. Within each selection category the candidate with the largest p_{T} has priority over the others.

The two dominant production mechanisms of a scalar boson are gluon fusion (ggF) and EW production, the latter dominated by vector boson fusion (VBF) with a small contribution of production in association with an EW boson ZH or WH (VH). We define the parameter f_{VBF} as the fraction of the EW production cross section with respect to the total cross section. The results are given for two scenarios: f_{VBF} floated, and $f_{VBF} = 1$. In the expected result, the two scenarios correspond to ggF and VBF production modes, respectively. To increase the sensitivity to the different production modes, events are categorized into VBF and inclusive types. Furthermore, since a large fraction of signal events is enriched with b quark jets due to the presence of $\text{Z} \to \text{b}\bar{\text{b}}$ decays, a dedicated category is defined. The definitions are as follows:

- **VBF-tagged** requires two additional and forward jets besides those from the hadronic decays of the Z boson candidate; a mass dependent criterion based on a dedicated discriminant defined for this category is applied;
- b **tagged** consists of the remaining events with two b tagged jets (in the resolved case) or two b tagged subjets from the hadronic Z boson candidate;
- **Untagged** consists of the remaining events.

The invariant mass of ZZ and a dedicated discriminant separating signal and background distributions are compared between observation and expected background to set limits on the production cross section.

Further details of the Run-2 analysis, including simulation samples, background estimation methods, systematic uncertainties, and different interpretations are described in Ref [19]. Only details of direct relevance to the projection of the Run-2 analysis are documented in the following.

A projection of this analysis is carried out by scaling all the signal and background processes to an integrated luminosity of 3000 fb^{-1}, expected to be collected at the high-luminosity LHC (HL-LHC). The projection does not account for the small cross section change due to the expected increase of the center of mass energy from Run-2 (13) TeV to HL-LHC (14 TeV). The upgrade and the expected performance of the CMS detector are described in the following section, and in detail in the Technical Proposal and the Technical Design Reports for the Phase-2 Upgrade of the CMS Detector [20–24]. Special care is taken to use realistic assumptions for the development of systematic uncertainties at high luminosity. The results are presented in terms of cross section limits on a heavy resonance decaying to a Z boson pair.

2 Upgraded CMS detector

The CMS detector [25] will be substantially upgraded in order to fully exploit the physics potential offered by the increase in luminosity at the HL-LHC [26], and to cope with the demanding operational conditions at the HL-LHC [20–24]. The upgrade of the first level hardware trigger (L1) will allow for an increase of L1 rate and latency to about 750 kHz and 12.5 μs, respectively, while in case of the high-level software trigger (HLT) its upgrade will allow the HLT rate to be increased to 7.5 kHz. The entire pixel and strip tracker detectors will be replaced to increase the granularity, reduce the material budget in the tracking volume, improve the radiation hardness, and extend the geometrical coverage and provide efficient tracking up to pseudorapidities of about $|\eta| = 4$. The muon system will be enhanced by upgrading the electronics of the existing cathode strip chambers (CSC), resistive plate chambers (RPC) and drift tubes (DT). New muon detectors based on improved RPC and gas electron multiplier (GEM) technologies will be installed to add redundancy, increase the geometrical coverage up to about $|\eta| = 2.8$, and improve the trigger and reconstruction performance in the forward region. The barrel electromagnetic calorimeter (ECAL) will feature the upgraded front-end electronics that will be able to exploit the information from single crystals at the L1 trigger level, to accommodate trigger latency and bandwidth requirements, and to provide an increased sampling rate of 160 MHz. The hadronic calorimeter (HCAL) consists in the barrel region of brass absorber plates and plastic scintillator layers, read out by hybrid photodiodes (HPDs), which will be replaced with silicon photomultipliers (SiPMs). The endcap electromagnetic and hadron calorimeters will be replaced with a new combined sampling calorimeter (HGCal) that will provide highly-segmented spatial information in both transverse and longitudinal directions, as well as high-precision timing information. Finally, the addition of a new timing detector for

minimum ionizing particles (MTD) in both barrel and endocap region is envisaged to provide capability for 4-dimensional reconstruction of interaction vertices that will allow to significantly offset the CMS performance degradation due to high PU rates.

A detailed overview of the CMS detector upgrade program is presented in Ref. [20–24], while the expected performance of the reconstruction algorithms and pile-up mitigation with the CMS detector is summarised in Ref. [27].

3 Extrapolation procedure

This projection assumes that the CMS experiment will have a similar level of detector and triggering performance during the HL-LHC operation as it provided during the LHC Run 2 period [20–24]. The results of projection are presented for different assumptions based on the size of systematic uncertainties that is estimated for HL-LHC:

- **"Run 2 systematic uncertainties" scenario:** This scenario assumes that performance of the experimental methods at the HL-LHC will be unchanged with respect to the LHC Run 2 period, and there will be no significant improvement in the quantitative theoretical understanding of relevant physics effects. All experimental and theoretical systematic uncertainties are assumed to be unchanged with respect to the ones in the reference Run 2 analysis, and kept constant with integrated luminosity.
- **"YR18 systematics uncertainties" scenario:** This scenario assumes that there will be further advances in both experimental methods and theoretical descriptions of relevant physics effects. Theoretical uncertainties are assumed to be reduced by a factor two with respect to the ones in the reference Run 2 analysis. For experimental systematic uncertainties, it is assumed that those will be reduced by the square root of the integrated luminosity until they reach a defined lower limit based on estimates of the achievable accuracy with the upgraded detector [27].

In these scenarios, the statistical error from simulation is assumed to be negligible, under the assumption that sufficiently large simulation samples will be available by the time the HL-LHC becomes operational. For all scenarios, the intrinsic statistical uncertainty in the measurement is expected to scale by $1/\sqrt{\mathrm{L}}$, where L is the projection integrated luminosity divided by that of the reference Run 2 analysis.

Table 1 summarises the Run 2 uncertainties as well as the "YR18 systematics uncertainties" scenario. Systematic uncertainties in the identification and isolation efficiencies for electrons and muons are expected to be reduced to around 0.5%. The uncertainty in the overall jet energy scale (JES) is expected to reach around 1% precision for jets with $p_{\mathrm{T}} > 30\,\mathrm{GeV}$, driven primarily by improvements for the absolute scale and jet flavour calibrations. For the identification of b-tagged jets, the uncertainty in the selection efficiency of b(c) quarks, and in misidentifying a light jet is expected to reach around 1% precision. The uncertainty in the integrated luminosity of the data sample could be reduced down to 1% by a better understanding of the calibration and fit models employed in its determination, and making use of the finer granularity and improved electronics of the upgraded detectors.

Among other systematic uncertainties, the theoretical uncertainty from higher order QCD corrections on the ggZZ background and the signal is the most dominant for the ggF search. It is expected that theoretical description of these processes will be improved, thus the uncertainty is scaled by 0.5. The next important ones are the shape and yield uncertainties of the Z+jets background. They are determined from a data control region and are scaled with $1/\sqrt{L}$ in YR18

Table 1: The sources of systematic uncertainty where minimum values are applied in "YR18 systematics uncertainties" scenario. Systematic uncertainties of the reference Run 2 analysis are described in Ref. [19].

Source	Run 2 uncertainty	Projection minimum uncertainty
Lepton selection efficiency	4–8%	0.5%
Lepton ID	1–10%	0.5%
Jet energy scale, resolution	1–10%	1%
b-tagging	5–7%	1%
Integrated luminosity	2.5%	1%

scenario. It is expected that at HL-LHC, the Z+jets background will have huge statistics, and the understanding of it will be at the percent level. Another important uncertainty is Z+jets fake rates. In the Run-2 analysis, they are derived from LO MC samples, and differences with repect to the NLO samples with limited statistics are assigned as systematic uncertainty. It is expected that larger statistics sample will be produced in the future or higher order description will be available to reduce this systematics uncertainty, thus it is scaled by 0.5 in YR18 scenario.

4 Results

The m_{ZZ} distribution of the events expected at 3000 fb^{-1} is shown in Figure 1. Figure 2 shows upper limits at the 95% confidence level (CL) on the $pp \to X \to ZZ$ cross section $\sigma_X \times \mathcal{B}_{X\to ZZ}$ as a function of m_X for a narrow resonance whose Γ_X is much smaller than the experimental resolution.

We follow the modified frequentist prescription [28–30] (CLs method), and an asymptotic approach with the profile likelihood ratio as the test statistic is used to estimate the upper limits at 95% confidence level. Systematic uncertainties are treated as nuisance parameters and profiled using log-normal priors.

The analysis uses $2\ell 2q$ final state to look for a scalar Higgs in the mass range of 550– 3000 GeV. It is the most sensitive channel above mass 700 GeV, while $2\ell 2\nu$ final state is the most sensitive for the intermediate region of 500–700 GeV. The exclusion limit for the cross section of the scalar decaying to a pair of Z bosons is 0.7–5 fb for the VBF production mode and 0.8–9 fb for the ggF production mode. This represents a factor of 10 improvement with respect to the results obtained using Run2 data. The differences between the two scenarios are minor and mostly present in the low mass region. It is because the search will still be limited by statistical uncertainties. The systematic uncertainties in this search have mild effects. If no $1/\sqrt{L}$ scaling is applied, the difference in the limit is 10% at low mass and almost none in the high mass region. The results for wide resonances are not given in this note for simplicity. The Run-2 result has shown that the excluded cross section for a 30% width resonance will be 40% higher at 1 TeV, compared to a narrow resonance assumption.

References

[1] S. L. Glashow, "Partial-symmetries of weak interactions", *Nucl. Phys.* **22** (1961) 579, doi:10.1016/0029-5582(61)90469-2.

[2] F. Englert and R. Brout, "Broken symmetry and the mass of gauge vector mesons", *Phys. Rev. Lett.* **13** (1964) 321, doi:10.1103/PhysRevLett.13.321.

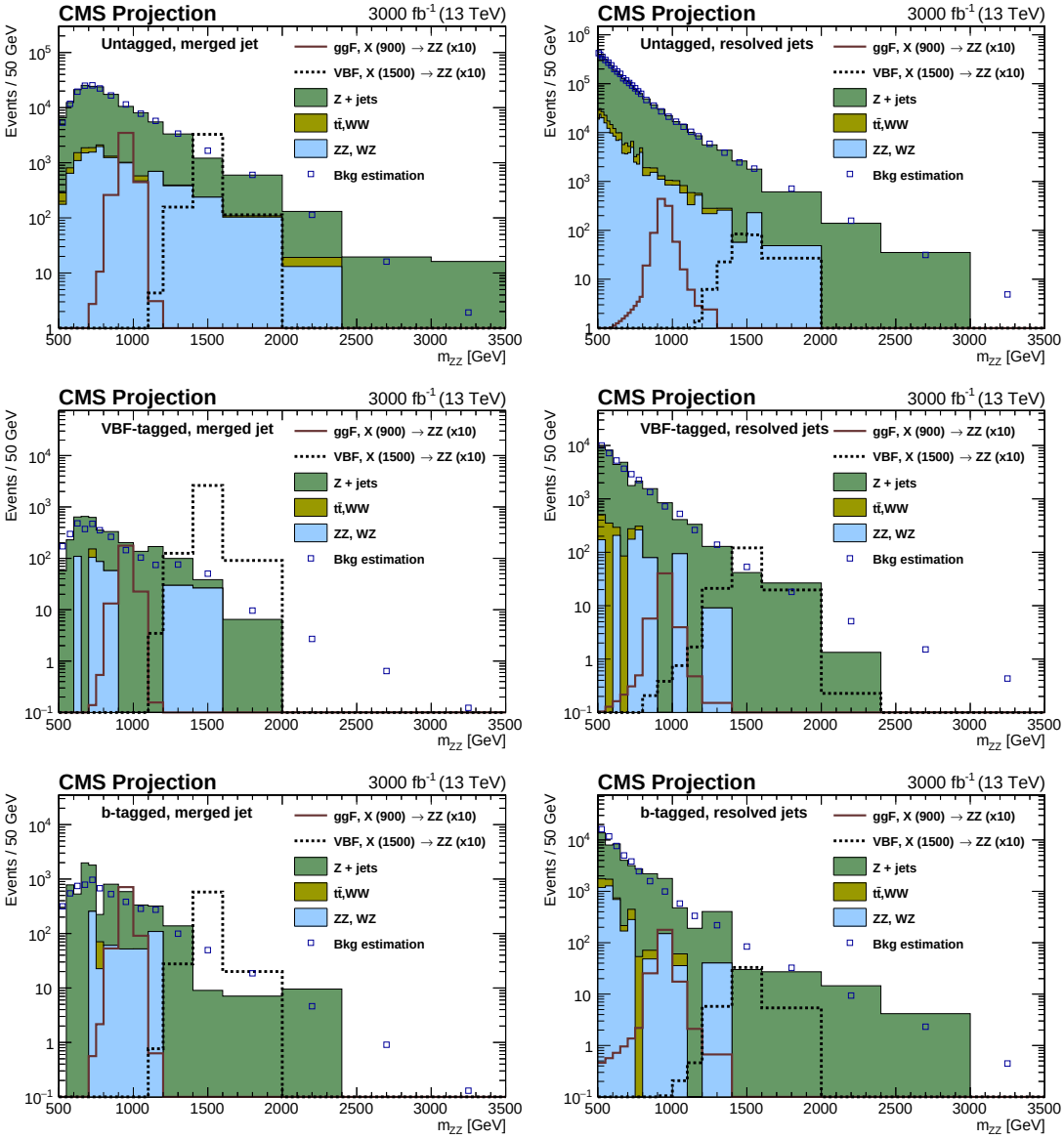

Figure 1: Distributions of the invariant mass m_{ZZ} in the signal region expected at 3000 fb^{-1}, for the merged (left) and resolved (right) case in the different categories. The stacked histograms are the expected backgrounds from simulation. The blue points refer to the sum of background estimates derived from control samples. Examples of a 900 GeV ggF signal and a 1500 GeV VBF signal are given. The cross section corresponds to 10 times the excluded limit.

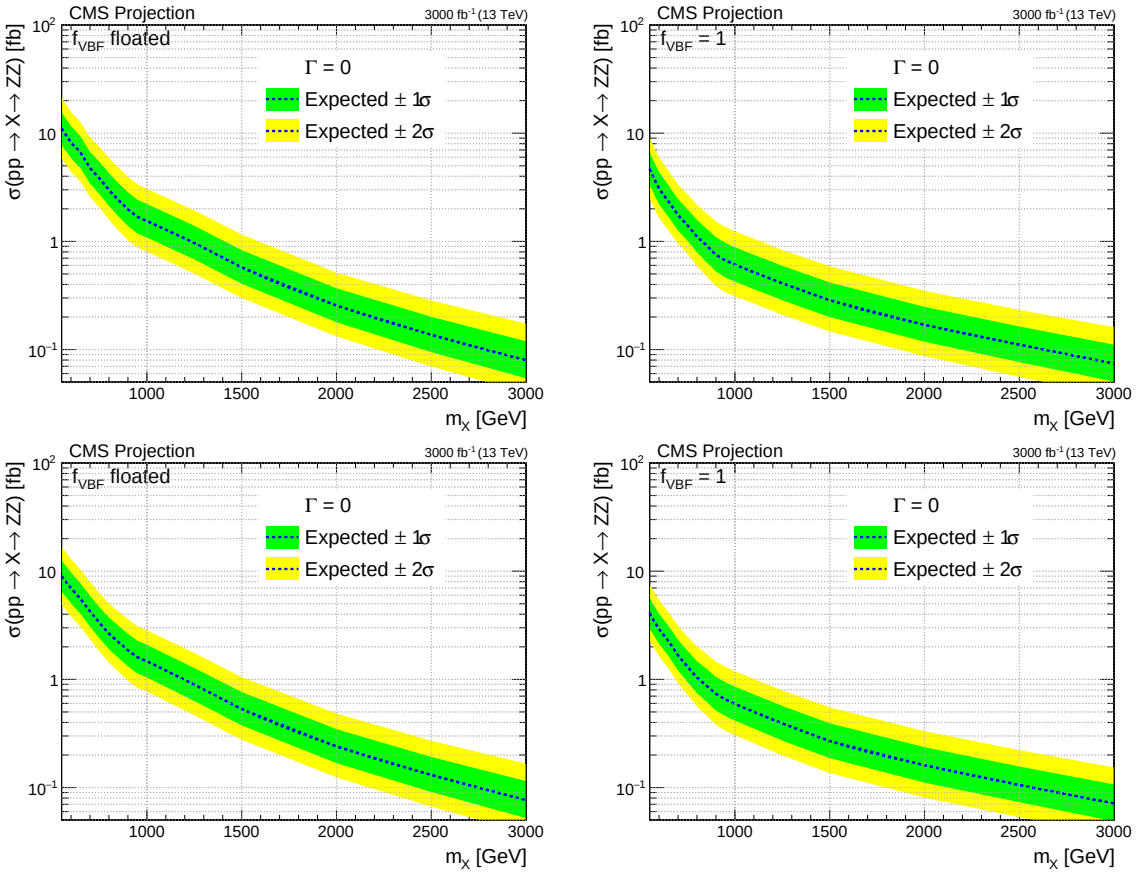

Figure 2: Expected upper limits at the 95% CL on the pp $\rightarrow$ X $\rightarrow$ ZZ cross section as a function of m_X, with f_{VBF} as a free parameter (left) and fixed to 1 (right). Scenario 1 (top) and scenario 2 (bottom) are shown. The scalar particle X is assumed to have a narrower decay width than the detector resolution. The results are shown for the 2ℓ2q channel.

[3] P. W. Higgs, "Broken symmetries, massless particles and gauge fields", *Phys. Lett.* **12** (1964) 132, doi:10.1016/0031-9163(64)91136-9.

[4] P. W. Higgs, "Broken symmetries and the masses of gauge bosons", *Phys. Rev. Lett.* **13** (1964) 508, doi:10.1103/PhysRevLett.13.508.

[5] G. S. Guralnik, C. R. Hagen, and T. W. B. Kibble, "Global conservation laws and massless particles", *Phys. Rev. Lett.* **13** (1964) 585, doi:10.1103/PhysRevLett.13.585.

[6] S. Weinberg, "A model of leptons", *Phys. Rev. Lett.* **19** (1967) 1264, doi:10.1103/PhysRevLett.19.1264.

[7] A. Salam, "Weak and electromagnetic interactions", in *Elementary particle physics: relativistic groups and analyticity*, N. Svartholm, ed., p. 367. Almqvist & Wiksell, Stockholm, 1968. Proceedings of the eighth Nobel symposium.

[8] ATLAS Collaboration, "Observation of a new particle in the search for the standard model Higgs boson with the ATLAS detector at the LHC", *Phys. Lett. B* **716** (2012) 1, doi:10.1016/j.physletb.2012.08.020, arXiv:1207.7214.

[9] CMS Collaboration, "Observation of a new boson at a mass of 125 GeV with the CMS experiment at the LHC", *Phys. Lett. B* **716** (2012) 30, doi:10.1016/j.physletb.2012.08.021, arXiv:1207.7235.

[10] CMS Collaboration, "Observation of a new boson with mass near 125 GeV in pp collisions at $\sqrt{s}$ = 7 and 8 TeV", *JHEP* **06** (2013) 081, doi:10.1007/JHEP06(2013)081, arXiv:1303.4571.

[11] CMS Collaboration, "Study of the mass and spin-parity of the Higgs boson candidate via its decays to Z boson pairs", *Phys. Rev. Lett.* **110** (2013) 081803, doi:10.1103/PhysRevLett.110.081803, arXiv:1212.6639.

[12] CMS Collaboration, "Measurement of the properties of a Higgs boson in the four-lepton final state", *Phys. Rev. D* **89** (2014) 092007, doi:10.1103/PhysRevD.89.092007, arXiv:1312.5353.

[13] CMS Collaboration, "Constraints on the spin-parity and anomalous HVV couplings of the Higgs boson in proton collisions at 7 and 8 TeV", *Phys. Rev. D* **92** (2015) 012004, doi:10.1103/PhysRevD.92.012004, arXiv:1411.3441.

[14] ATLAS Collaboration, "Evidence for the spin-0 nature of the Higgs boson using ATLAS data", *Phys. Lett. B* **726** (2013) 120, doi:10.1016/j.physletb.2013.08.026, arXiv:1307.1432.

[15] ATLAS Collaboration, "Study of the spin and parity of the Higgs boson in diboson decays with the ATLAS detector", *Eur. Phys. J. C* **75** (2015) 476, doi:10.1140/epjc/s10052-015-3685-1, arXiv:1506.05669.

[16] G. C. Branco et al., "Theory and phenomenology of two-Higgs-doublet models", *Phys. Rept.* **516** (2012) 1, doi:10.1016/j.physrep.2012.02.002, arXiv:1106.0034.

[17] C. Caillol, B. Clerbaux, J.-M. Frére, and S. Mollet, "Precision versus discovery: A simple benchmark", *Eur. Phys. J. Plus* **129** (2014) 93, doi:10.1140/epjp/i2014-14093-3, arXiv:1304.0386.

[18] ATLAS Collaboration, "Combination of searches for heavy resonances decaying into bosonic and leptonic final states using 36 fb^{-1} of proton-proton collision data at $\sqrt{s} = 13$ TeV with the ATLAS detector", *Phys. Rev.* **D98** (2018), no. 5, 052008, doi:10.1103/PhysRevD.98.052008, arXiv:1808.02380.

[19] CMS Collaboration, "Search for a new scalar resonance decaying to a pair of Z bosons in proton-proton collisions at $\sqrt{s} = 13$ TeV", *JHEP* **06** (2018) 127, doi:10.1007/JHEP06(2018)127, arXiv:1804.01939.

[20] CMS Collaboration, "Technical Proposal for the Phase-II Upgrade of the CMS Detector", Technical Report CERN-LHCC-2015-010. LHCC-P-008. CMS-TDR-15-02, 2015.

[21] CMS Collaboration, "The Phase-2 Upgrade of the CMS Tracker", Technical Report CERN-LHCC-2017-009. CMS-TDR-014, 2017.

[22] CMS Collaboration, "The Phase-2 Upgrade of the CMS Barrel Calorimeters Technical Design Report", Technical Report CERN-LHCC-2017-011. CMS-TDR-015, 2017.

[23] CMS Collaboration, "The Phase-2 Upgrade of the CMS Muon Detectors", Technical Report CERN-LHCC-2017-012. CMS-TDR-016, 2017.

[24] CMS Collaboration, "The Phase-2 Upgrade of the CMS Endcap Calorimeter", Technical Report CERN-LHCC-2017-023. CMS-TDR-019, 2017.

[25] CMS Collaboration, "The CMS Experiment at the CERN LHC", *JINST* **3** (2008) S08004, doi:10.1088/1748-0221/3/08/S08004.

[26] G. Apollinari et al., "High-Luminosity Large Hadron Collider (HL-LHC) : Preliminary Design Report", doi:10.5170/CERN-2015-005.

[27] CMS Collaboration, "Expected performance of the physics objects with the upgraded CMS detector at the HL-LHC", Technical Report CMS-NOTE-2018-006. CERN-CMS-NOTE-2018-006, CERN, Geneva, Dec, 2018.

[28] T. Junk, "Confidence level computation for combining searches with small statistics", *Nucl. Instrum. Meth. A* **434** (1999) 435, doi:10.1016/S0168-9002(99)00498-2, arXiv:hep-ex/9902006.

[29] A. L. Read, "Presentation of search results: The CL_s technique", *J. Phys. G* **28** (2002) 2693, doi:10.1088/0954-3899/28/10/313.

[30] G. Cowan, K. Cranmer, E. Gross, and O. Vitells, "Asymptotic formulae for likelihood-based tests of new physics", *Eur. Phys. J. C* **71** (2011) 1554, doi:10.1140/epjc/s10052-011-1554-0, arXiv:1007.1727. [Erratum: doi:10.1140/epjc/s10052-013-2501-z].